Eur Biophys J (2010) 39:1251–1259
DOI 10.1007/s00249-010-0578-y

ORIGINAL PAPER

Dynamics of strand passage catalyzed by topoisomerase II

Ping Xie

Received: 10 November 2009 / Revised: 17 December 2009 / Accepted: 13 January 2010 / Published online: 3 February 2010

Abstract DNA topoisomerase II is a homodimeric molecular machine that uses ATP hydrolysis to untangle DNA by passing one double-stranded DNA duplex (T-segment) through another double-stranded duplex (G-segment). However, despite extensive studies, the dynamics of ATP-dependent T-transport is still not very clear. Here, based on the proposal that transport of the T-segment through the transiently cleaved G-segment and the opened C-gate of the enzyme is via a free diffusion mechanism, the dynamics of T-transport are studied theoretically. Our results show that, to complete passage of the strand with nearly 100% efficiency, the C-gate is required to open by a width that is only slightly larger than the width of DNA duplex and for a time shorter than 100 μs in the presence of several k_BT binding affinities of the T-segment for the B′ domains. The results are implied by our understanding of the opening and closing dynamics of the C-gate. Moreover, the dependence of chemomechanical coupling efficiency on degrees of DNA supercoiling by gyrases can also be explained by using our results. On the basis of these theoretical results and previous experimental data, a modified two-gate model for chemomechanical coupling of the topoisomerase II enzyme is proposed.

Keywords DNA transport · DNA topology · Chemomechanical coupling mechanism · Gyrase · Molecular machine · Model

Introduction

Type II DNA topoisomerase (topo II) is an enzyme that catalyzes the ATP-dependent transport of one DNA double helix through another, thus resolving topological problems, for example supercoiling, knotting, and catenation, that occur during DNA replication, transcription, recombination, chromosome segregation, and chromosome condensation (Wang 1996; Burden and Osheroff 1998; Champoux 2001; Corbett and Berger 2004; Schoeffler and Berger 2005). Eukaryotic topo II is a symmetric homodimer and each monomer is composed of three principal domains: an N-terminal ATPase domain, and the B′ and A′ domains that constitute the DNA cleavage–relegation core (Fig. 1a) (Wigley et al. 1991; Berger et al. 1996; Collins et al. 2009). In the absence of ATP, the two monomers contact each other primarily in the region within the A′ domain, with the open ATPase domains and B′ domains allowing DNA binding (Roca et al. 1996), whereas binding of the ATP or ATP analog leads to closing of the ATPase and B′ domains (Wigley et al. 1991; Berger et al. 1996; Roca and Wang 1992; Olland and Wang 1999; Ali et al. 1993, 1995; Hu et al. 2002; Gardiner et al. 1998; Brino et al. 2000; Classen et al. 2003; Wei et al. 2005; Lamour et al. 2002; Fass et al. 1999; Lindsley and Wang 1993).

Based on extensive biochemical and structural studies, a general two-gate model for the action of topo II has been proposed; this is briefly stated as follows (Corbett and Berger 2004; Schoeffler and Berger 2005; Roca et al. 1996; Berger and Wang 1996; Bates and Maxwell 2007; Mueller

Electronic supplementary material The online version of this article (doi:10.1007/s00249-010-0578-y) contains supplementary material, which is available to authorized users.

P. Xie (✉)
Laboratory of Soft Matter Physics, Institute of Physics, Chinese Academy of Sciences, 100190 Beijing, China
e-mail: pxie@aphy.iphy.ac.cn

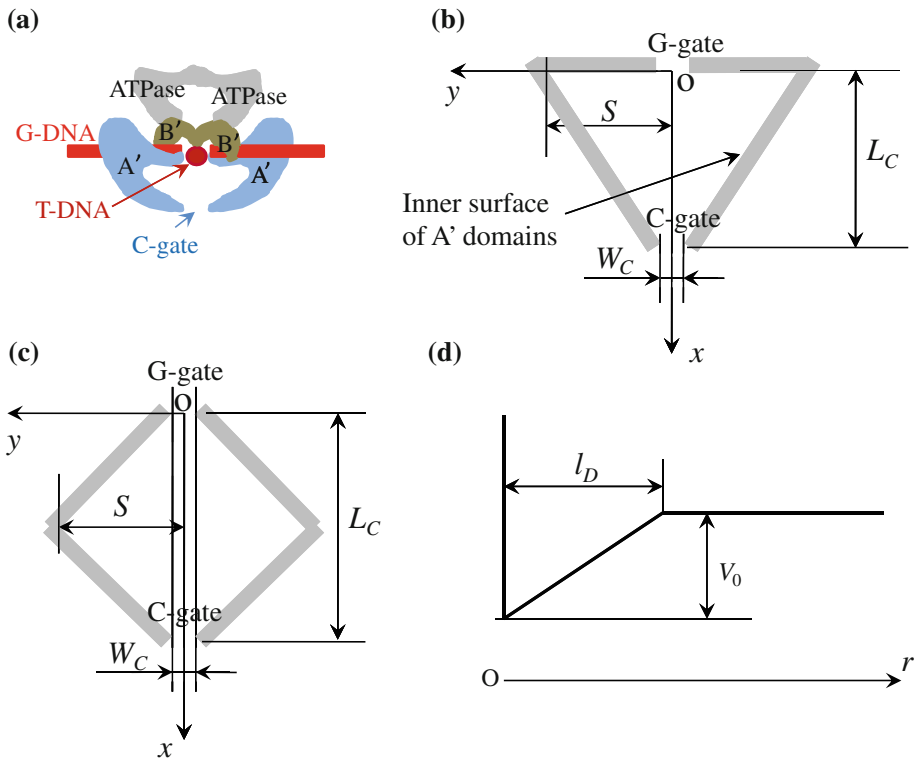

Fig. 1 **a** Conformation of topo II upon G-segment cleaving after closure of the ATPase and B′ domains. **b** Schematic diagram of the triangular form of the inner-surface shape of the A′ domains. **c** Schematic diagram of the rhombic form of the inner-surface shape of the A′ domains. **d** Interaction potential, $V(r)\left(r=\sqrt{x^2+y^2}\right)$, between the T-segment and B′ domains after the closure of the ATPase and B′ domains

and Herschalg 2008). The enzyme first binds to two different DNA segments. One segment, termed the gate or G-segment, binds to the cleavage/relegation region. The other DNA segment, termed the transported or T-segment, binds and is trapped inside the enzyme upon binding of two ATP molecules that leads to closing of the ATPase domains and B′ domains. The closure of the ATPase and B′ domains activates G-segment cleavage. Hydrolysis of the first ATP takes place, which induces transport of the T-segment through the break in the G-segment. The T-segment is then transported through the C-terminal exit gate (C-gate) of the enzyme. The ATPase and B′ domains stay closed even after hydrolysis of the first ATP and can reopen when the second ATP is hydrolyzed and the hydrolysis products are released to allow another round of catalytic reaction. However, in the model, how the T-segment is transported through the C-gate that is spatially far away (about 5 nm) from the G-segment is not clear. A proposal was that, after crossing the G-DNA segment, the T-DNA segment is then expelled from the C-gate by the A′–A′ dimer interface at the hinge of the closed clamp (Roca 2009). However, because transport of the T-segment is under over-damped condition, this would involve too large a conformational change of the dimer interface. Moreover, the opening and closing dynamics of the C-gate are not clear.

In this work, we propose that transport of the T-segment through the transiently cleaved G-DNA segment and the opened C-gate is via a free diffusion mechanism. Using this free diffusion model, we theoretically study the dynamics of T-transport without the external force acting on it, which corresponds approximately to the working conditions of conventional topo II during the decatenation of linked catenanes or DNA untangling, and with the external force acting on it, which corresponds approximately to the working conditions of gyrase during the introduction of a negative supercoil into supercoiled DNA. The results without the external force show that, to complete passage of the strand with a nearly 100% efficiency, the C-gate is required to open by a width that is only slightly larger than the width of DNA duplex and for a time much shorter than the mean nucleotide-transition time. The results are implicated in our understanding of the opening and closing dynamics of the C-gate. The results with the external force can give a good explanation of the experimental results of the effect of degrees of DNA supercoiling on the chemo-mechanical coupling efficiency of gyrase.

Methods

In this work, we use the two-gate model and focus on the dynamics of transport of the T-segment through the C-gate after the G-segment is cleaved following closure of the ATPase and B′ domains, as shown in Fig. 1a. We assume that the C-gate opens transiently accompanying the

opening of the G-gate. Moreover, it is argued that the exit of the T-segment from the C-gate is not because it is expelled by the A′–A′ dimer interface; rather, we assume that it is a result of free diffusion driven by thermal noise.

For simplicity of analysis, based on the available structures (Berger et al. 1996; Fass et al. 1999), two approximate forms of the inner surface of the A′ domains are considered: one has a triangular form, as shown in Fig. 1b, and the other one has a rhombic form, as shown in Fig. 1c. Taking the coordinate *xoy* shown in Fig. 1b or c, the movement of the T-segment is confined in the region satisfying the condition of $x \geq 0$ and $|y| \leq (S - d/2) - (S - W_C/2)x/L_C$ for the triangular form, where S is the distance defined as shown in Fig. 1b, W_C is the width of the C-gate, d is the width of DNA duplex, and L_C is the distance between the C-gate and the T-segment-binding site on the B′ domains. For the rhombic form, the movement of the T-segment is confined in the region satisfying the condition: $|y| \leq (W_C - d)/2 + (2S - W_C)x/L_C$ when $0 \leq x < L_C/2$ and $|y| \leq [2S - (W_C - d)/2 - d] + (W_C - 2S)x/L_C$ when $L_C/2 \leq x \leq L_C$. From the available structure (Berger et al. 1996; Fass et al. 1999), we approximately have $S = 4$ nm and $L_C = 5$ nm. In this work we take $W_C = d + \Delta$, where Δ is larger than 0.

After the G-segment is cleaved and the G and C-gates are opened, the movement of the T-segment along the x and y directions in the over-damped environment can be described by the following Langevin equations

$$\Gamma \frac{dx}{dt} = -\frac{\partial V(r)}{\partial x} + \xi_x(t), \tag{1a}$$

$$\Gamma \frac{dy}{dt} = -\frac{\partial V(r)}{\partial y} + \xi_y(t), \tag{1b}$$

where Γ is the frictional drag coefficient and $V(r)\left(r = \sqrt{x^2 + y^2}\right)$ is the interaction potential of the T-segment with the B′ domains. $\xi_m(t)$ $(m = x, y)$ is the fluctuating Langevin force, with $\langle \xi_m(t) \rangle = 0$ and $\langle \xi_m(t)\xi_n(t') \rangle = 2k_B T \cdot \Gamma \cdot \delta_{mn}\delta(t - t')$, where k_B is the Boltzmann constant and $T = 300$ K. Approximating the T-segment as a polymer having diameter d and length l, with $d/l \ll 1$, the drag coefficient can be calculated by use of the equation $\Gamma = \frac{4\pi\eta l}{\ln(l/d) + 2\ln 2 - 1/2}$ (Wiggins et al. 1998). The interaction potential $V(r)$ can be approximately shown in Fig. 1d, with the potential depth V_0 and the interaction distance l_D that is approximately equal to the Debye length in solution.

Equations 1a and 1b are solved numerically by using the stochastic Runge–Kutta algorithm as used elsewhere (Xie et al. 2007; Xie 2008). In our calculation, we take $d = 2$ nm and $l = 100$ nm, which gives $\Gamma = 2.62 \times 10^{-10}$ kg s^{-1}. Because inside cell the Debye length is about 1 nm, we take $l_D = 1$ nm in the calculation. The T-segment is initially positioned at $(x, y) = (0, 0)$. Because values of Δ and V_0 are not available, we take them as variables in this work. In our calculation, when the T-segment moves to position at $x = L_C$ and $|y| < \Delta/2$, it is considered that passage of the strand is complete and the time taken for the T-segment to move to the position at $x = L_C$ and $|y| < \Delta/2$ corresponds to the strand-passage time.

Results

In the main text, we only present results for the triangular form of the inner surface of the A′ domains (Fig. 1b). The results for the rhombic form of the inner surface of the A′ domains (Fig. 1c) are presented in the supplementary material. Comparison of the results for the two forms shows that different forms of the inner surface of the A′ domains have slightly different effects on the dynamics of T-transport. The rhombic form shows slightly smaller mean strand-passage time than the triangular form, especially for small values of Δ.

Dynamics of T-transport without external force

In Fig. 2 we show two typical results for the trace of movement of the T-segment with $\Delta = 0.2$ nm and different values of V_0. It is seen that, after the G and C-gates become open, which occurs at $t = 0$, the T-segment rapidly exits from the C-gate as a result of the thermal noise, especially for small values of V_0. The strand-passage time distributions for $\Delta = 0.2$ nm and two different values of V_0 are shown in Fig. 3. It is seen that the distribution can be fitted well by a single exponential, $A \cdot \exp(-t/T_d)$, where A is a constant and T_d is the mean strand-passage time.

To see the effect of Δ on passage of the strand, in Fig. 4 we show the calculated results of the mean strand-passage time as a function of Δ for different values of V_0. As expected, the mean strand-passage time decreases with increasing Δ. However, it is interesting to see that the mean strand-passage time only decreases slowly with increasing Δ: for example, when Δ increases tenfold (from 0.1 to 1 nm), the mean strand-passage time decreases by a factor of two, approximately, only. Even if the opening width of the C-gate is only slightly wider than the width of the DNA duplex, e.g., $\Delta \leq 0.2$ nm, the mean strand-passage time is also very short. This implies that to ensure complete passage of the strand the C-gate is required to open by a width that is only slightly larger than the width of DNA duplex.

To see the effect of V_0 on strand passage, in Fig. 5a we show the calculated results of the mean strand-passage time as a function of V_0 for different values of Δ (unfilled symbols). From the figure it is apparent that the mean strand-passage time increases significantly with increasing

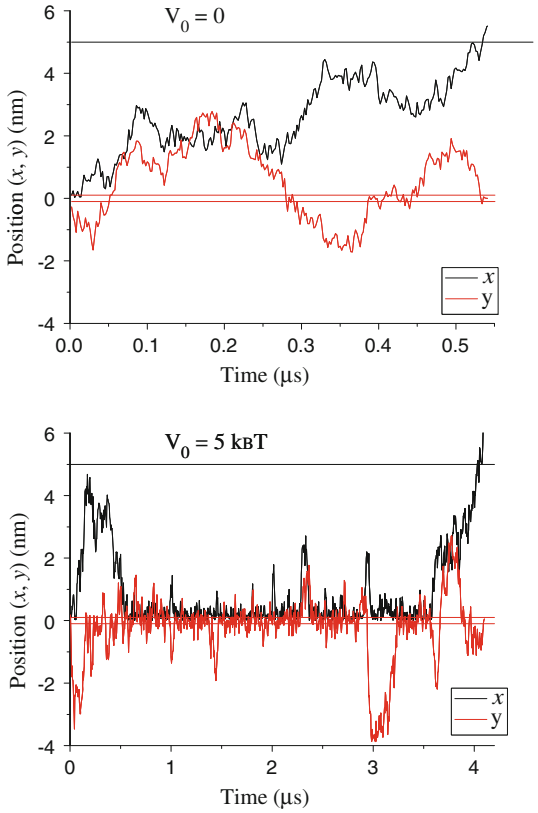

Fig. 2 Typical results for the trace of movement of the T-segment with $\Delta = 0.2$ nm and different values of V_0. $F_{ext} = 0$. The *straight black line* corresponds to $x = L_C = 5$ nm whereas the *two straight red lines* correspond to $y = -\Delta/2 = -0.1$ nm and $y = \Delta/2 = 0.1$ nm, respectively

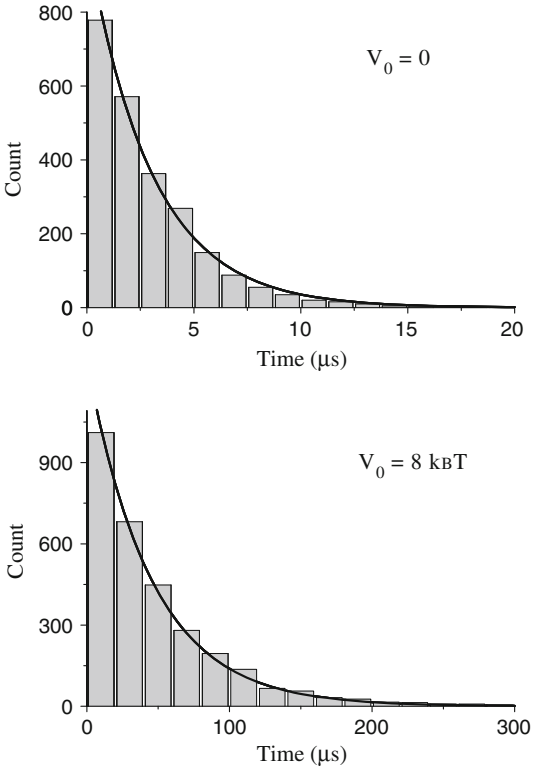

Fig. 3 Strand-passage time distributions for $\Delta = 0.2$ nm and different values of V_0, fitted with single exponential, $A \cdot \exp(-t/T_d)$, of time constants $T_d \approx 1.6$ and 23 μs for $V_0 = 0$ and 8 k_BT, respectively, $F_{ext} = 0$

V_0. However, it is noted that, even for a very large value of $V_0 = 10\ k_BT$, the mean strand-passage time is shorter than 200 μs. From the single-exponential time distribution, $f(t) = (1/T_d)\exp(-t/T_d)$ (Fig. 3), it is easily obtained from Fig. 5a that for 99% probability of the T-segment exiting from the C-gate the results for required opening time of the C-gate as a function of V_0 are as shown in Fig. 5b. It is seen that, for $\Delta = 0.2$ nm and $V_0 = 0$, the opening time of the C-gate is required to be only about 12.3 μs; for $V_0 = 5\ k_BT$, the opening time is required to be only about 35 μs; and for V_0 as large as 10 k_BT, the opening time is required to be only about 1.18 ms.

When the T-segment is allowed to diffuse in one dimension only (i.e., along the x direction), the analytical form of the mean strand-passage time can be obtained. The Fokker–Planck equation corresponding to Eq. 1a has the form $\frac{\partial P(x,t)}{\partial t} = \frac{1}{\Gamma}\frac{\partial}{\partial x}\left[\frac{\partial V(x)}{\partial x}P(x,t)\right] + D\frac{\partial^2 P(x,t)}{\partial^2 x}$, where $D = k_BT/\Gamma$. The mean first-passage time or the mean strand-passage time for the T-segment to diffuse from $x = 0$ to $x = L_C$ can be calculated by use of the equation $T_d = (1/D)\int_0^{L_C} \mathrm{d}y \exp[V(y)/(\Gamma D)] \int_0^y \exp[-V(z)/(\Gamma D)]\mathrm{d}z$ (Gardiner 1983). By integration of this equation with the form of $V(x)$ given in Fig. 1c, we obtain:

$$T_d = \frac{l_D\Gamma}{V_0}\left\{\frac{l_D\Gamma D}{V_0}\left[\exp\left(\frac{V_0}{\Gamma D}\right) - 1\right] - l_D\right\} + \frac{l_D\Gamma}{V_0}\left[\exp\left(\frac{V_0}{\Gamma D}\right) - 1\right](L_C - l_D) + \frac{(L_C - l_D)^2}{2D}. \quad (2)$$

When $V_0 = 0$, Eq. 2 becomes:

$$T_d = \frac{L^2}{2D}. \quad (3)$$

Using Eqs. 2 and 3, the analytical results of T_d versus V_0 are also shown in Fig. 5a (line). In order to check our numerical method, in Fig. 5a we also show the numerical results for diffusion along the x direction only (filled squares) by solving Eq. 1a. The numerical results are identical with the analytical ones. Comparing the results for the 1D-diffusion case with those for the 2D-diffusion case, it is seen that, for $V_0 < 4\ k_BT$, diffusion along y direction slightly increases the mean strand-passage time; whereas for $V_0 > 5\ k_BT$, allowing diffusion along the y direction decreases the mean strand-passage time. This can be understood as follows. For $V_0 < 4\ k_BT$, the T-segment can be considered to diffuse freely. Diffusion to position

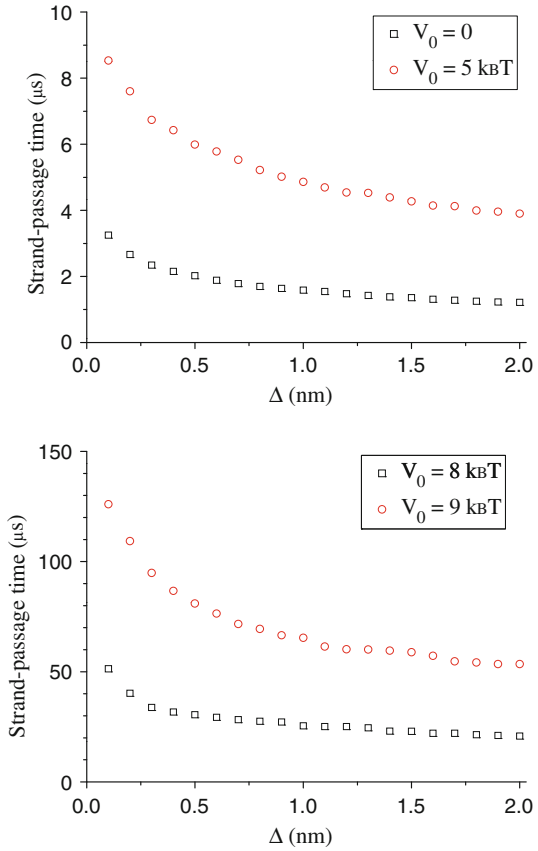

Fig. 4 Mean strand-passage time as a function of Δ for different values of V_0. $F_{ext} = 0$

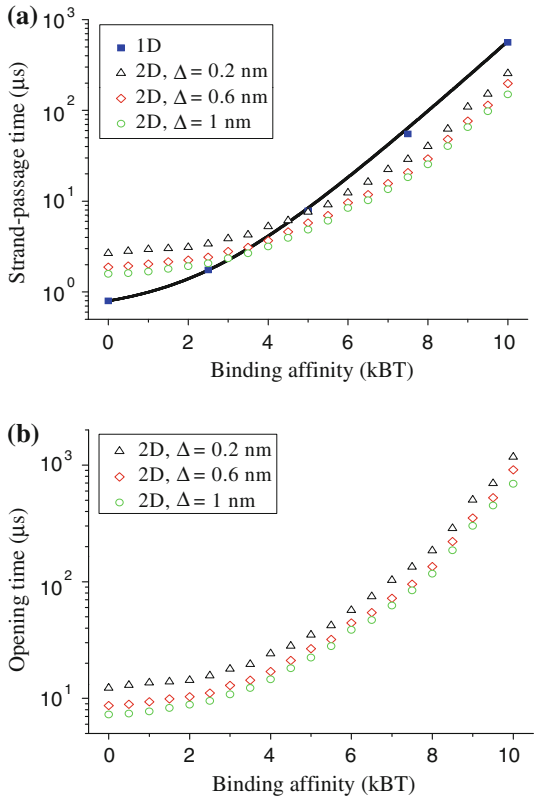

Fig. 5 Results with no external force acting on the T-segment, i.e., with $F_{ext} = 0$. **a** Mean strand-passage time as a function of V_0 for different values of Δ. *Unfilled symbols* represent the numerical results for the 2D-diffusion case. *Filled squares* represent the numerical results for the 1D-diffusion case. *Solid line* is the analytical result for the 1D-diffusion case. **b** Required opening time of the C-gate as a function of V_0 for different values of Δ

($x < L_C$, $|y| > \Delta/2$) increases the time for the T-segment to arrive at the C-gate positioned at ($x = L_C$, $|y| < \Delta/2 < S - d/2$). In fact, we have checked that, by taking $W_C = d + \Delta = 2S$, the numerically obtained mean strand-passage time for the 2D-diffusion case with $V_0 = 0$ becomes equal to that for the 1D-diffusion case with $V_0 = 0$. However, for $V_0 > 5\ k_BT$, most of the time taken for the T-segment to arrive at the C-gate is the time to stay at the potential well with depth V_0. Allowing motion in two dimensions decreases the time to escape from the potential well compared with motion in one dimension only, thus giving a smaller strand-passage time.

From Figs. 4 and 5, we conclude that, to complete strand passage with an efficiency of 99%, the C-gate is required to open by a width that is only slightly larger than the width of DNA duplex and for a time shorter than 100 μs for $V_0 < 6.5\ k_BT$. Even for a very large value of $V_0 = 10\ k_BT$, the C-gate is only required to open for a short time of the order of 1 ms.

Dynamics of T-transport with external force

So far we have studied T-transport dynamics with no external force acting on the T-segment, which corresponds approximately to the working conditions of conventional topo II during the decatenation of linked catenanes or DNA untangling.

To see the effect of external force, we added a term, $-F_{ext}$, on the right-hand side of Eq. 1a, where F_{ext} is defined as positive when it points along the $-x$ direction or points upwards. In Fig. 6a we show calculated results for the mean strand-passage time as a function of F_{ext} for different values of Δ, with $V_0 = 5\ k_BT$. As expected, the mean strand-passage time increases significantly with increasing upward external force. Next, we use these results for mean strand-passage time to study the strand-passage efficiency. As the opening time of the C-gate of a topoisomerase has a given value independent of the external force acting on the T-segment, for example, we take here the opening time of the C-gate as that for which the strand-passage efficiency under no external force is 99%. Then, from Fig. 6a, the calculated results for strand-passage efficiency versus F_{ext} are shown in Fig. 6b. From Fig. 6 we see that, although the strand-passage time depends on Δ at large values of F_{ext}, the strand-passage

efficiency is insensitive to variation of Δ. Moreover, it is interesting to see from Fig. 6b that the chemomechanical coupling efficiency decreases significantly with increasing upward external force. At zero or downward external force, the efficiency is nearly 100%; for upward external force of only $F_{ext} = 2$ pN, the efficiency decreases to approximately 60%; for $F_{ext} = 3$ pN, the efficiency decreases to approximately 36%; at $F_{ext} = 4$ pN, the efficiency decreases to a value smaller than 20%. On the other hand, it is known that, during introduction of a negative supercoil into positively supercoiled DNA, by transporting the T-segment through the G-segment, the positively supercoiled DNA will facilitate this transport. In contrast, introduction of a further negative supercoil into negatively supercoiled DNA will resist transport of the T-segment. In other words, the T-segment experiences a facilitating force (corresponding to the downward external force) when a negative supercoil is introduced into positively supercoiled DNA; whereas it experiences a resisting force (corresponding to the upward external force) when a negative supercoil is introduced into negatively supercoiled DNA and, as σ (the linking difference) decreases, the resisting force increases. Thus, the results of Fig. 6b can give an explanation of the experimental results for gyrase obtained by Bates et al. (1996), who showed that the chemomechanical coupling efficiency approached 100% with positively supercoiled DNA as the substrate and decreased steadily with moderate degrees of negatively supercoiling.

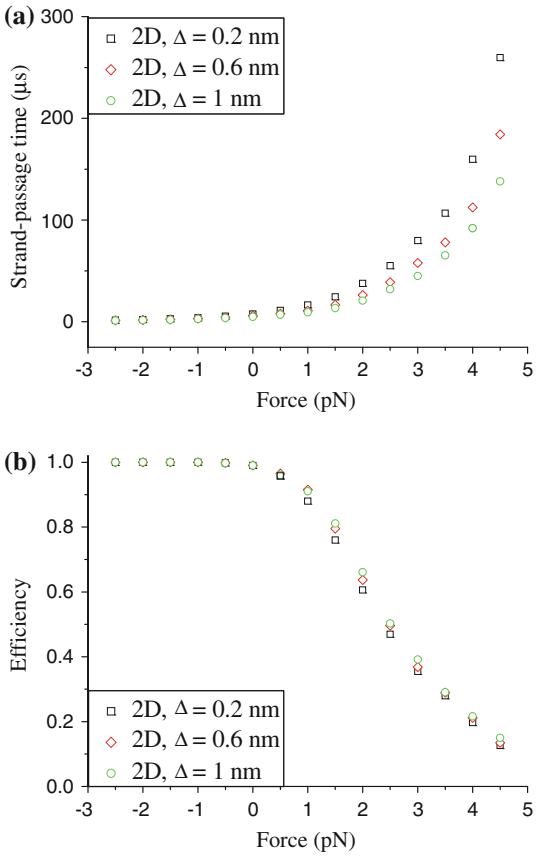

Fig. 6 Results with external force F_{ext} acting on the T-segment for $V_0 = 5\ k_BT$ and different values of Δ. **a** Mean strand-passage time versus F_{ext}. **b** Chemomechanical coupling efficiency versus F_{ext}

Discussion

Our results for the dynamics of T-transport without external force acting on it show that, to complete passage of the strand with a nearly 100% efficiency, the C-gate is only required to open transiently for a short time, for example, for $V_0 = 5\ k_BT$, the C-gate is only required to open for a short time of approximately 30 μs (Fig. 5b and Fig. S5b). In contrast, from previous experimental data on nucleotide-transition rates (Baird et al. 1999), we know that the mean nucleotide-transition time is of the order of seconds. Thus, if binding by topo II is such that transition of the nucleotide induces closing of the C-gate, the C-gate would open for a time of the order of seconds, which is much longer than 30 μs. In order to reduce the probability of the exited T-segment re-entering the inner of the A′ domains, the C-gate should open for a time as short as is required for the T-segment to exit from it. Thus, it is reasonable to assume that, after the C-gate is opened, it re-closes elastically, with a time of the order of 10 μs, rather than closing of the C-gate being induced by transition of the nucleotide. In other words, it is assumed that the closed conformation of the C-gate corresponds to that having the minimum free energy in either the nucleotide-free or nucleotide-bound state. Opening of the G-gate induces the two A′ domains to be apart, which in turn induces, elastically, opening of the C-gate. The C-gate then re-closes elastically to remain in the minimum free-energy conformation. This argument is consistent with puzzling experimental results which showed that, after ATP or AMPPNP binds, the G-gate opens (Smiley et al. 2007) and passage of the strand can occur (Roca and Wang 1994; Baird et al. 1999), but in steady AMPPNP state the C-gate is closed (Roca and Wang 1992).

Previous experimental results showed that the ATP hydrolysis rate is about 40 s^{-1} and the Pi-release rate is very high, whereas the DNA decatenation rate (or the strand-passage rate) is about 7.1 s^{-1} in the presence of ATP (Baird et al. 1999). However, our results show that the strand-passage time, which is in the order of 10 μs, is very short. We thus infer that the measured strand-passage rate of about 7.1 s^{-1} corresponds approximately to the G-segment-cleavage rate and that hydrolysis of one ATP precedes DNA transport. This is consistent with the experimental data of Baird et al. (1999). On the other hand,

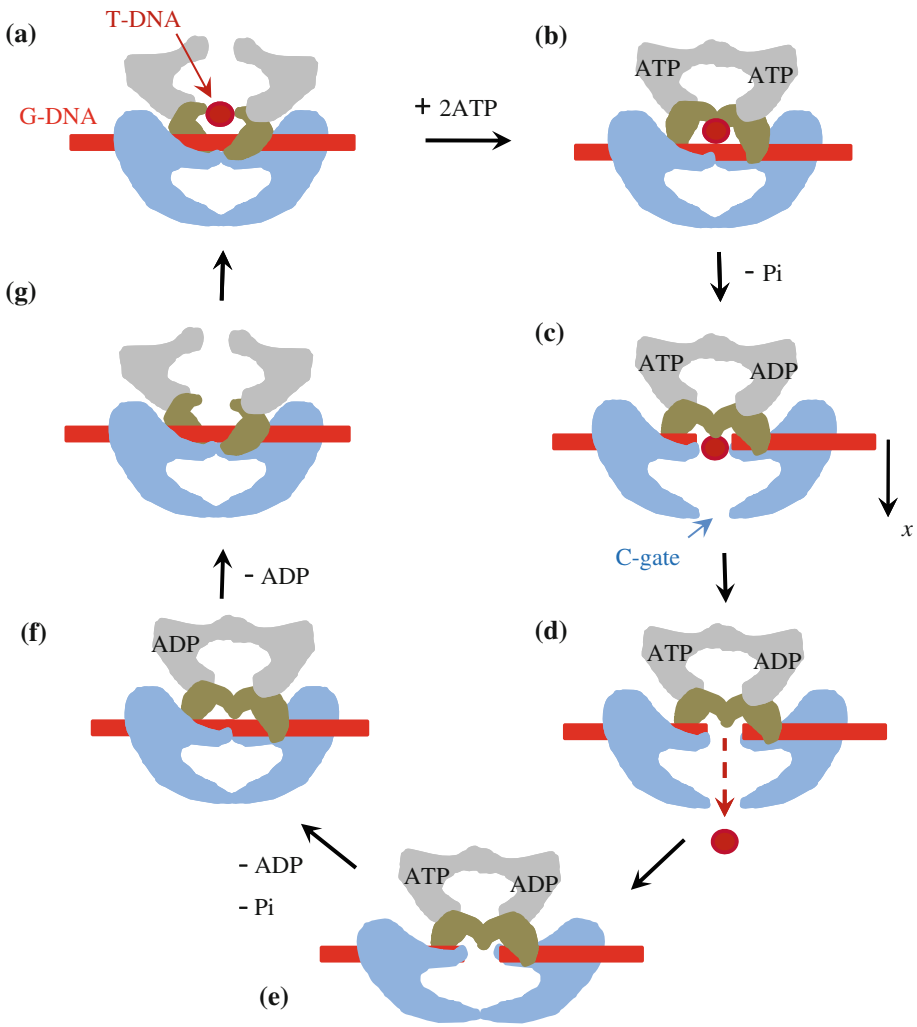

Fig. 7 Schematic illustration of chemomechanical coupling of topo II in the presence of ATP (see text for detailed description)

previous experimental data showed that the strand-passage rate in the presence of AMPPNP is much smaller than that in the presence of ATP (Baird et al. 1999). We thus infer that hydrolysis of one ATP can further accelerate the rate of G-segment-cleavage. Based on these deductions, previous experimental data (Wigley et al. 1991; Berger et al. 1996; Mueller and Herschalg 2008; Roca and Wang 1992, 1994; Olland and Wang 1999; Ali et al. 1993, 1995; Hu et al. 2002; Gardiner et al. 1998; Brino et al. 2000; Classen et al. 2003; Wei et al. 2005; Lamour et al. 2002; Fass et al. 1999; Lindsley and Wang 1993; Harkins and Lindsley 1998; Harkins et al. 1998; Smiley et al. 2007; Baird et al. 1999; Skouboe et al. 2003; Vaughn et al. 2005; Morais Cabral et al. 1997) and our current theoretical data, we thus propose a modified two-gate model for the chemomechanical coupling of the topo II enzyme, which is stated as follows.

We begin with the nucleotide-free topo II binding to a crossover between the G and T-segments (Fig. 7a). The binding of the G-segment by topo II should cause significant bending of the G-segment (Dong and Berger 2007). For simplicity, we have not shown this bending here. The binding of two ATP molecules leads to closing of the ATPase and B′ domains, which activates G-segment cleavage (Fig. 7b). However, before the G-segment is cleaved, the G-gate in the two A′ domains is prevented from opening by its strong interaction with the G-segment. Then one ATP molecule is hydrolyzed and Pi is released rapidly, which further activates G-segment cleavage. After the G-segment is cleaved, the G-gate is allowed to open, which in turn induces opening of the C-gate (Fig. 7c). This allows diffusion of the T-segment inside the inner of the two A′ domains and its exit from the opened C-gate (Fig. 7d). The C-gate then re-closes elastically, thus preventing the exited T-segment from re-entering the inner of the two A′ domains (Fig. 7e). After turnover of the first ATP molecule, hydrolysis of second ATP molecule, and then rapid Pi release, the G-gate becomes closed, which religates the cleaved G-segment (Fig. 7f). Release of second ADP leads to opening of the ATPase and B′ domains to allow another round of catalysis (Fig. 7g).

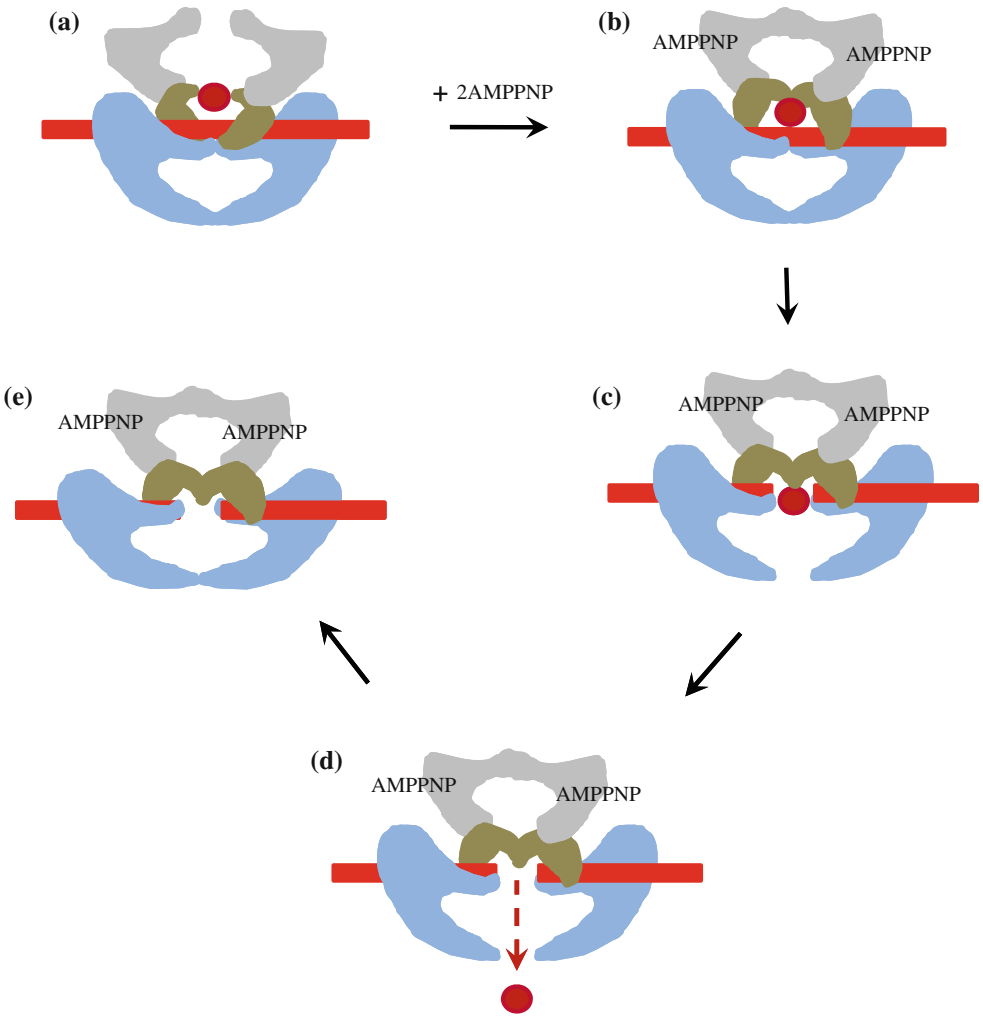

Fig. 8 Schematic illustrations of a single turnover strand passage mediated by topo II in the presence of AMPPNP (see text for detailed description)

A single turnover strand passage in the presence of AMPPNP is shown schematically in Fig. 8. The nucleotide-free topo II binds to a crossover between the G and T-segments (Fig. 8a). The binding of two AMPPNP molecules leads to closing of the ATPase and B′ domains, which activates G-segment cleavage (Fig. 8b). After the G-segment is cleaved, the G-gate opens, which in turn induces opening of the C-gate (Fig. 8c). Free diffusion of the T-segment causes it to exit from the opened C-gate (Fig. 8d). The C-gate then re-closes elastically, thus preventing the exited T-segment from re-entering the inner of the two A′ domains (Fig. 8e).

Acknowledgments This work was supported by the National Natural Science Foundation of China (Grant No. 10974248).

References

Ali JA, Jackson AP, Howells AJ, Maxwell A (1993) The 43-kilodalton N-terminal fragment of the DNA gyrase B protein hydrolyzes ATP and binds coumarin drugs. Biochemistry 32:2717–2724

Ali JA, Orphanides G, Maxwell A (1995) Nucleotide binding to the 43-kilodalton N-terminal fragment of the DNA gyrase B protein. Biochemistry 34:9801–9808

Baird CL, Harkins TT, Morris SK, Lindsley JE (1999) Topoisomerase II drives DNA transport by hydrolyzing one ATP. Proc Natl Acad Sci USA 96:13685–13690

Bates AD, Maxwell A (2007) Energy coupling in type II topoisomerases: why do they hydrolyze ATP? Biochemistry 46:7929–7941

Bates AD, O'Dea MH, Gellert M (1996) Energy coupling in *Escherichia coli* DNA gyrase: the relationship between nucleotide binding, strand passage, and DNA supercoiling. Biochemistry 35:1408–1416

Berger JM, Wang JC (1996) Recent developments in DNA topoisomerase II structure and mechanism. Curr Opin Struct Biol 6:84–90

Berger JM, Gamblin SJ, Harrison SC, Wang JC (1996) Structure and mechanism of DNA topoisomerase II. Nature 379:225–232

Brino L, Urzhumtsev A, Mousli M, Bronner C, Mitschler A, Oudet P, Moras D (2000) Dimerization of *Escherichia coli* DNA-gyrase B provides a structural mechanism for activating the ATPase catalytic center. J Biol Chem 275:9468–9475

Burden DA, Osheroff N (1998) Mechanism of action of eukaryotic topoisomerase II and drugs targeted to the enzyme. Biochim Biophys Acta 1400:139–154

Champoux JJ (2001) DNA topoisomerases: structure, function, and mechanism. Annu Rev Biochem 70:369–413

Classen S, Olland S, Berger JM (2003) Structure of the topoisomerase II ATPase region and its mechanism of inhibition by the chemotherapeutic agent ICRF-187. Proc Natl Acad Sci USA 100:10629–10634

Collins TRL, Hammes GG, Hsieh T-S (2009) Analysis of the eukaryotic topoisomerase II DNA gate: a single-molecule FRET and structural perspective. Nucleic Acids Res 37:712–720

Corbett KD, Berger JM (2004) Structure, molecular mechanisms, and evolutionary relationships in DNA topoisomerases. Annu Rev Biophys Biomol Struct 33:95–118

Dong KC, Berger JM (2007) Structural basis for gate-DNA recognition and bending by type IIA topoisomerases. Nature 450:1201–1205

Fass D, Bogden CE, Berger JM (1999) Quaternary changes in topoisomerase II may direct orthogonal movement of two DNA strands. Nat Struct Biol 6:322–326

Gardiner CW (1983) Handbook of stochastic methods for physics, chemistry and the natural sciences. Springer, Berlin

Gardiner LP, Roper DI, Hammonds TR, Maxwell A (1998) The N-terminal domain of human topoisomerase II-alpha is a DNA-dependent ATPase. Biochemistry 37:16997–17004

Harkins TT, Lindsley JE (1998) Pre-steady-state analysis of ATP hydrolysis by *saccharomyces cerevisiae* DNA topoisomerase II. 1. A DNA-dependent burst in ATP hydrolysis. Biochemistry 37:7292–7298

Harkins TT, Lewis TJ, Lindsley JE (1998) Pre-steady-state analysis of ATP hydrolysis by *saccharomyces cerevisiae* DNA topoisomerase II. 2. Kinetic mechanism for the sequential hydrolysis of two ATP. Biochemistry 37:7299–7312

Hu T, Sage H, Hsieh TS (2002) ATPase domain of eukaryotic DNA topoisomerase II. J Biol Chem 277:5944–5951

Lamour V, Hoermann L, Jeltsch JM, Oudet P, Moras D (2002) An open conformation of the *Thermus thermophilus* gyrase B ATP-binding domain. J Biol Chem 277:18947–18953

Lindsley JE, Wang JC (1993) Study of allosteric communication between protomers by immunotagging. Nature 361:749–750

Morais Cabral JH, Jackson AP, Smith CV, Shikotra N, Maxwell A, Liddington RC (1997) Crystal structure of the break age-reunion domain of DNA gyrase. Nature 388:903–906

Mueller F, Herschalg D (2008) Coupling between ATP binding and DNA cleavage by DNA topoisomerase II: a unified kinetic and structural mechanism. J Biol Chem 283:17463–17476

Olland S, Wang JC (1999) Catalysis of ATP hydrolysis by two NH_2-terminal fragments of yeast DNA topoisomerase II. J Biol Chem 274:21688–21694

Roca J (2009) Topoisomerase II: a fitted mechanism for the chromatin landscape. Nucleic Acids Res 37:721–730

Roca J, Wang JC (1992) The capture of a DNA double helix by an ATP-dependent protein clamp: a key step in DNA transport by type II DNA topoisomerases. Cell 71:833–840

Roca J, Wang JC (1994) DNA transport by a type II DNA topoisomerase: evidence in favor of a two-gate mechanism. Cell 77:609–616

Roca J, Berger JM, Harrison SC, Wang JC (1996) DNA transport by a type II topoisomerase: direct evidence for a two-gate mechanism. Proc Natl Acad Sci USA 93:4057–4062

Schoeffler AJ, Berger JM (2005) Recent advances in understanding structure-function relationships in the type II topoisomerase mechanism. Biochem Soc Trans 33:1465–1470

Skouboe C, Bjergbaek L, Oestergaard VH, Larsen MK, Knudsen BR, Andersen AH (2003) A human topoisomerase II α heterodimer with only one ATP binding site can go through successive catalytic cycles. J Biol Chem 278:5768–5774

Smiley RD, Collins TRL, Hammes GG, Hsieh T-S (2007) Single-molecule measurements of the opening and closing of the DNA gate by eukaryotic topoisomerase II. Proc Natl Acad Sci USA 104:4840–4845

Vaughn J, Huang S, Wessel I, Sorensen TK, Hsieh T, Jensen LH, Jensen PB, Sehested M, Nitiss JL (2005) Stability of the topoisomerase II closed clamp conformation may influence DNA-stimulated ATP hydrolysis. J Biol Chem 280:11920–11929

Wang JC (1996) DNA topoisomerases. Annu Rev Biochem 65:635–692

Wei H, Ruthenburg AJ, Bechis SK, Verdine GL (2005) Nucleotide-dependent domain movement in the ATPase domain of a human type IIA DNA topoisomerase. J Biol Chem 280:37041–37047

Wiggins CH, Riveline D, Ott A, Goldstein RE (1998) Trapping and wiggling: elastohydrodynamics of driven microfilaments. Biophys J 74:1043–1060

Wigley DB, Davies GJ, Dodson EJ, Maxwell A, Dodson G (1991) Crystal structure of an N-terminal fragment of the DNA gyrase B protein. Nature 351:624–629

Xie P (2008) Stepping behavior of two-headed kinesin motors. Biochim Biophys Acta 1777:1195–1202

Xie P, Dou S-X, Wang P-Y (2007) Processivity of single-headed kinesin motors. Biochim Biophys Acta 1767:1418–1427